

## Femtosecond Two-Dimensional Raman Spectroscopy of Liquid Water

Stephen Palese,<sup>†</sup> Joseph T. Buontempo, Lynn Schilling, William T. Lotshaw,<sup>‡</sup>  
Yoshitaka Tanimura, Shaul Mukamel, and R. J. Dwayne Miller\*

Department of Chemistry and the Institute of Optics, University of Rochester, Rochester, New York 14627

Received: June 30, 1994; In Final Form: October 15, 1994<sup>Ⓢ</sup>

Higher-order Raman spectra for water are calculated using the Brownian oscillator model for the nuclear degrees of freedom which is constrained to fit the spectral density obtained between 0 and 1000  $\text{cm}^{-1}$ . Assuming a static distribution, both fifth- and seventh-order processes are capable of distinguishing the homogeneous and inhomogeneous character of the spectral density. Through temperature-dependent heterodyne optical Kerr effect studies, an upper limit ( $150 \pm 30$  fs extrapolated to 100 °C) for the homogeneous lifetime in liquid water was established. The intermediate fifth-order case was analyzed to incorporate this dynamically evolving distribution of local environments and indicates that, even for a system as complex as water, higher-order field correlations can access information on its dynamic structure.

### I. Introduction

The delineation of the vibrational line shapes of liquids into homogeneous or inhomogeneous classifications has been the subject of numerous experimental and theoretical studies.<sup>1,2</sup> Inhomogeneously broadened linewidths arise from the different transition frequencies associated with energetically and dynamically distinct local environments. Such line shapes carry no information about the dynamics of the system. Homogeneous broadening mechanisms, however, are directly related to the system dynamics through fluctuations in these local environments. This latter information is critical to a detailed description of liquid dynamics and time scale issues surrounding the basis sets used to model liquid modes and relaxation phenomena.

The first studies of liquid modes in the low-frequency range focused on the use of frequency domain infrared and Raman spectroscopies.<sup>3</sup> Recent developments in spectroscopic methods have significantly augmented the study of these modes in the 0–1000  $\text{cm}^{-1}$  frequency range through femtosecond time-resolved coherent spectroscopies.<sup>4,5</sup> However, the information content in both the frequency domain and time domain experiments is the same. The main difference between the time and frequency domain approaches is that time domain experiments are generally more sensitive to frequencies less than 100  $\text{cm}^{-1}$ , whereas frequency domain experiments are easier to extend to frequencies above 500  $\text{cm}^{-1}$ . While these experiments provide information about intramolecular and intermolecular degrees of freedom which are both local and collective in nature, neither approach can directly distinguish between homogeneous and inhomogeneous broadening in the associated spectroscopic transitions. In the low-frequency range relevant to liquid dynamics ( $<1000 \text{ cm}^{-1}$ ), there are many different modes which spectrally overlap. The resultant line shape can be fit to various models, but these models always have underlying assumptions regarding the inhomogeneity of the distribution such that an unambiguous correlation of the line shapes to the bath dynamics is not possible.

Nonlinear techniques such as photon echoes are, however, capable of dissecting the line shape into homogeneous and

inhomogeneous contributions.<sup>6</sup> In the low-frequency range appropriate to liquids, such experiments can be conducted using either far-infrared (terahertz) or Raman scattering processes. The fact that an experiment is optically nonlinear is not a sufficient criterion for this capability. Loring *et al.*<sup>7</sup> have shown that the electronically off-resonant coherent Raman experiments which contain only one time variable (e.g., optical Kerr effect (OKE) and coherent anti-Stokes Raman spectroscopies) are formally equivalent to linear spectroscopies and that multitime (multiple pulse) Raman experiments, analogous to the photon echo, are necessary to distinguish between homogeneous and inhomogeneous mechanisms. It is therefore informative to study theoretically (through numerical calculations) the multiple-pulse Raman spectroscopies associated with these higher-order experiments.

The present analysis of the higher-order Raman response of liquids has focused on water as the model system since it is expected to have large inhomogeneous contributions at frequencies less than 1000  $\text{cm}^{-1}$  based on molecular dynamic simulations.<sup>8</sup> In addition, water has historically been considered one of the most important liquids due primarily to its central role in biological processes. The highly hydrogen-bonded network nested within the fluid structure gives water the unique properties which sustain biological processes.<sup>9</sup> For example, the strong driving force for hydrogen bond formation is primarily responsible for the occurrence of hydrophobic and hydrophilic moieties in protein architecture. The propensity of water to form hydrogen-bonded structures with different numbers of molecules and orientations greatly contributes to the large inhomogeneous vibrational distribution of this liquid. Considerable theoretical efforts have been directed toward understanding the dynamic structure of water using various approaches.<sup>10</sup> Most recently, quenched normal mode and instant normal mode analyses have been conducted which focus on the low-frequency vibrational spectrum of water.<sup>10–12</sup> Higher-order experiments will provide more information about the liquid structure and dynamics than the linear experiments and will also determine the time scale in which the system can be viewed as inhomogeneous and hence amendable to a modal analysis. However, *a priori*, it is unclear that concepts developed from previous higher-order experiments of single oscillator distributions can be applied to the intermolecular spectrum of a liquid as complex as water. This system has many different dynamical degrees of freedom with potentially different frequency distributions which all spectrally overlap within the pulse bandwidth and therefore contribute to

<sup>†</sup> Department of Physics and Astronomy.

<sup>‡</sup> General Electric Research and Development Center, P.O. Box 8, Schenectady, NY 12301.

\* To whom correspondence should be sent.

<sup>Ⓢ</sup> Abstract published in *Advance ACS Abstracts*, November 15, 1994.

the response function. Before the results of such experiments can be correlated to homogeneous and inhomogeneous contributions to the vibrational band shapes, a detailed analysis of the dependence of the higher-order response of water on time scale limits defining homogeneous and inhomogeneous dephasing is required. This work provides the necessary theoretical background for extending this approach to complex liquids and provides support for current experimental efforts in this area.<sup>13,14</sup>

## II. Theory and Numerical Calculations

Employing path integral techniques, Tanimura and Mukamel<sup>15</sup> have derived closed form expressions for the Raman response of a liquid subjected to a series of  $N$  electronically off-resonance laser pulses. The nuclear motions of the liquid were modeled by a multimode Brownian oscillator. Nuclear motions couple to the optical signal through the parametric dependence of the electronic polarizability ( $\alpha$ ) on the nuclear coordinates ( $q$ ) which was assumed to be exponential, i.e.,  $\alpha(q) = \alpha_0 \exp(aq)$ . All optical nonlinearities vanish if that dependence is linear; however, the exact form of the nonlinear coupling does not alter the general features of the calculation.<sup>15</sup> This model accounts for both homogeneous and inhomogeneous dephasing mechanisms and can be used either to represent specific nuclear coordinates or as a convenient parametrization. Expressing the signal amplitude and intensity of the  $N$ th-order process as  $R^{(N)}(\tau_{(N-1)/2}, \tau_{(N-3)/2}, \dots, \tau_1)$  and  $I^{(N)}(\tau_{(N-1)/2}, \tau_{(N-3)/2}, \dots, \tau_1)$  the Raman response functions (to first order in powers of  $a^2$ ) are given by

$$R^{(3)}(\tau_1) = (2\alpha_0^2 a^2 / \hbar) \int d\nu S_1(\nu) \sin(2\pi\nu\tau_1) \quad (1)$$

$$R^{(5)}(\tau_2, \tau_1) = (4\alpha_0^3 a^4 / \hbar^2) \int d\nu \int d\nu' S_2(\nu, \nu') \sin(2\pi\nu\tau_2) \times [\sin(2\pi\nu'\tau_1) + \sin(2\pi\nu'(\tau_1 + \tau_2))] \quad (2)$$

$$R^{(7)}(\tau_3, \tau_2, \tau_1) = (8\alpha_0^4 a^6 / \hbar^3) \int d\nu \int d\nu' \int d\nu'' S_3(\nu, \nu', \nu'') \times \sin(2\pi\nu\tau_3) [\sin(2\pi\nu'\tau_2) + \sin(2\pi\nu'(\tau_2 + \tau_3))] [\sin(2\pi\nu''\tau_1) + \sin(2\pi\nu''(\tau_1 + \tau_2)) + \sin(2\pi\nu''(\tau_1 + \tau_2 + \tau_3))] \quad (3)$$

where

$$S_1(\nu) = \int d\Gamma_\alpha S(\Gamma_\alpha) J(\nu; \Gamma_\alpha) \quad (4)$$

$$S_2(\nu, \nu') = \int d\Gamma_\alpha S(\Gamma_\alpha) J(\nu; \Gamma_\alpha) J(\nu'; \Gamma_\alpha) \quad (5)$$

$$S_3(\nu, \nu', \nu'') = \int d\Gamma_\alpha S(\Gamma_\alpha) J(\nu; \Gamma_\alpha) J(\nu'; \Gamma_\alpha) J(\nu''; \Gamma_\alpha) \quad (6)$$

In eqs 1–6,  $\Gamma_\alpha$  represents the set of parameters ( $\eta_\alpha, \nu_\alpha, \gamma_\alpha$ ) which specify each oscillator mode  $\alpha$ , where  $\eta_\alpha$  is the coupling strength,  $\nu_\alpha$  the central frequency, and  $\gamma_\alpha$  the relaxation rate.  $S(\Gamma_\alpha)$  is a distribution of  $\Gamma_\alpha$ .  $J(\nu; \Gamma_\alpha)$  refers to the theoretical spectral density function for a given realization of  $\Gamma_\alpha$ . The experimental spectral density obtained in e.g., femtosecond optical Kerr measurements, is obtained by summation of  $J$  over the distribution of  $\Gamma_\alpha$ , as implied in eqs 1 and 4. In the following analysis any distributions of  $\eta_\alpha$  and  $\gamma_\alpha$  are neglected, so that  $S(\Gamma_\alpha) \rightarrow S(\nu_\alpha)$  represents the frequency distribution responsible for traditional inhomogeneous dephasing.

We are interested in the ability of the  $N$ th-order nonlinear Raman process to discriminate between homogeneous and inhomogeneous dephasing mechanisms. We look first at the heterodyne (linear) OKE (OHD-OKE) signal which is given by  $R^{(3)}(\tau_1)$ . In the limit of purely homogeneous dephasing  $S(\nu_\alpha) = \delta(\nu_\alpha)$ , while in the limit of purely inhomogeneous dephasing

$J(\nu; \Gamma_\alpha) = \delta(\nu - \nu_\alpha)$  and thus

$$R_{ho}^{(3)}(\tau_1) = (2\alpha_0^2 a^2 / \hbar) \int d\nu J(\nu; \Gamma_\alpha) \sin(2\pi\nu\tau_1) \quad (7)$$

$$R_{in}^{(3)}(\tau_1) = (2\alpha_0^2 a^2 / \hbar) \int d\nu_\alpha S(\nu_\alpha) \sin(2\pi\nu_\alpha\tau_1) \quad (8)$$

In these two limiting cases,  $J(\nu; \Gamma_\alpha)$  and  $S(\nu_\alpha)$  determine  $R^{(3)}(\tau_1)$  in the same way, so it is not possible to directly distinguish between these physically distinct cases.<sup>23</sup> For the fifth-order process

$$R_{ho}^{(5)}(\tau_2, \tau_1) = (4\alpha_0^3 a^4 / \hbar^2) \int d\nu \int d\nu' J(\nu; \Gamma_\alpha) J(\nu'; \Gamma_\alpha) \times \sin(2\pi\nu\tau_2) [\sin(2\pi\nu'\tau_1) + \sin(2\pi\nu'(\tau_1 + \tau_2))] \quad (9)$$

$$R_{in}^{(5)}(\tau_2, \tau_1) = (4\alpha_0^3 a^4 / \hbar^2) \int d\nu_\alpha S(\nu_\alpha) \sin(2\pi\nu_\alpha\tau_2) \times [\sin(2\pi\nu_\alpha\tau_1) + \sin(2\pi\nu_\alpha(\tau_1 + \tau_2))] \quad (10)$$

Here  $J(\nu; \Gamma_\alpha)$  and  $S(\nu_\alpha)$  enter into the calculation of  $R^{(5)}(\tau_2, \tau_1)$  differently. Therefore, it is possible in principle to discriminate between the purely inhomogeneous and homogeneous limits in fifth order.

We also examine the special case of the seventh-order process given when the delay between the second and third pulses ( $\tau_2$ ) is zero. This implies a double interaction with the second pulse, such that the resulting nonlinear response function,  $R^{(7)}(\tau_3, 0, \tau_1)$ , determines the signal intensity analogous to the Raman echo experiment.

$$R_{ho}^{(7)}(\tau_3, 0, \tau_1) = (8\alpha_0^4 a^6 / \hbar^3) \left[ \int d\nu J(\nu; \Gamma_\alpha) \sin(2\pi\nu\tau_3) \right]^2 \times \int d\nu' J(\nu'; \Gamma_\alpha) [2 \sin(2\pi\nu'\tau_1) + \sin(2\pi\nu'(\tau_1 + \tau_3))] \quad (11)$$

$$R_{in}^{(7)}(\tau_3, 0, \tau_1) = (8\alpha_0^4 a^6 / \hbar^3) \int d\nu_\alpha S(\nu_\alpha) [\sin(2\pi\nu_\alpha\tau_3)]^2 \times [2 \sin(2\pi\nu_\alpha\tau_1) + \sin(2\pi\nu_\alpha(\tau_1 + \tau_3))] \quad (12)$$

Like the fifth-order experiment, it is possible to discriminate between the limiting cases in seventh order.

We have calculated  $R^{(3)}(\tau_1)$ ,  $R^{(5)}(\tau_2, \tau_1)$ , and  $R^{(7)}(\tau_3, 0, \tau_1)$  spectra of water in the homogeneous and inhomogeneous limits to examine the temporal features that should be expected. To do this, we obtain  $R^{(3)}(\nu)$  for water experimentally and then, following the procedure of Tanimura and Mukamel,<sup>15</sup> fit it with the parametrized function

$$R^{(3)}(\nu) = \sum_i \nu A_i C_i / (B_i^2 - \nu^2)^2 + \nu^2 C_i^2 \quad (13)$$

where  $A_i$ ,  $B_i$ , and  $C_i$  are parameters chosen to reproduce the experimental spectral density and  $\nu$  is the frequency in  $\text{cm}^{-1}$ . By taking the Fourier transforms of eqs 7 and 8, we see that  $R_{ho}^{(3)}(\nu) \propto J(\nu; \Gamma_\alpha)$  and  $R_{in}^{(3)}(\nu_\alpha) \propto S(\nu_\alpha)$  so that eq 13 is equal to  $J(\nu; \Gamma_\alpha)$  in the homogeneous limit and  $S(\nu_\alpha)$  in the inhomogeneous limit. In this way, we can deduce the higher-order signal dependence in the homogeneous limit by substituting eq 13 for  $J(\nu; \Gamma_\alpha)$  in eqs 7, 9, and 11 and in the inhomogeneous limit by substituting eq 13 for  $S(\nu_\alpha)$  in eqs 8, 10, and 12.

We obtained  $R^{(3)}(\nu)$  from the imaginary component of the Fourier transform of the deconvoluted, femtosecond OHD-OKE transient wave form.<sup>16</sup> The deconvoluted data are utilized to show the calculated nuclear contributions with minimal effects due to the finite spectral bandwidth of the excitation pulses. The fit of  $R^{(3)}(\nu)$  by eq 13 yielded the parameter values  $A_{1..6}$  (arbitrary units) (0.015, 0.13, 0.28, 0.67, 0.58, 1.00),  $B_{1..6}$  ( $\text{cm}^{-1}$ ) (40, 80, 200, 450, 570, 720), and  $C_{1..6}$  ( $\text{cm}^{-1}$ ) (170, 170, 170,

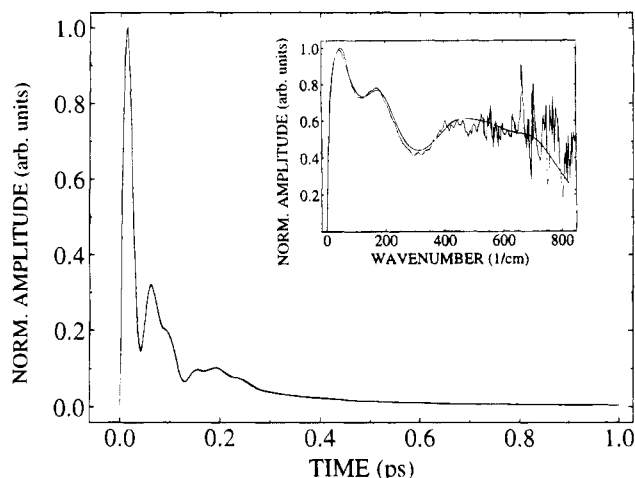


**Figure 1.** Third-order calculated deconvolved response for water. The homogeneous and inhomogeneous limits are equivalent in this order. The parameters for the calculation have been obtained by fitting the imaginary part of the FFT for the deconvolved, heterodyne, out-of-phase OKE response of water. The inset shows this frequency domain spectrum and the parametrized fit to six modes.

250, 250, 250). The correlations have also been calculated using  $R^{(3)}(\nu)$  obtained from the convolved experimental OHD-OKE spectrum and depolarized light scattering (DLS) spectra.<sup>16,17</sup> The qualitative results, to be discussed below, are essentially independent of which spectral density was utilized in the calculation.

The result for the calculation of the deconvolved  $R^{(3)}(\tau_1)$  response is shown in Figure 1. This result is of course identical for both the purely homogeneous and inhomogeneous limits. This figure illustrates the fitted response expected from nuclear contributions to the (OHD-OKE) signal and thus displays the time scale for the free induction decay of the ensemble of water oscillators. The calculations for the deconvolved  $I_{ho}^{(5)}(\tau_2, \tau_1)$ ,  $I_{in}^{(5)}(\tau_2, \tau_1)$ ,  $I_{ho}^{(7)}(\tau_3, 0, \tau_1)$ , and  $I_{in}^{(7)}(\tau_3, 0, \tau_1)$  are shown in Figures 2A, 2B, 3A, and 3B, respectively.

In these figures,  $\tau_1$  is the delay between excitation pulses and  $\tau_2$  ( $\tau_3$ ) is the delay of the probe defined from the application of the second (third) excitation. It is clear from these figures that the signal obtained in each limiting case is quite distinct. The fifth- and seventh-order inhomogeneous calculations show recurrences of the signal which are not present in the homogeneous responses. The recurrence at twice the excitation pulse separation is the classic signature for an inhomogeneously broadened distribution. The higher-order interaction of the nuclear polarization with the excitation field leads to a change in the phase of the induced polarization. For an inhomogeneous distribution, the spread in frequencies causes the nuclear polarization to decay more rapidly than the true homogeneous decay of the distinct sites within the distribution. The dephasing process evolves for a certain time interval ( $\tau_1$ ) and then is reversed by the second action of the fields. The rephasing process takes the same time as that allotted to the dephasing, such that the polarization monitored by the probe pulse exhibits a maximum at twice the excitation pulse separation ( $\tau_2 = \tau_1$ ). This maximum decays with the homogeneous decay time and is the traditional "echo" in photon and Raman echo studies of electronic and vibrational transitions, respectively. However, the distinction between the study of these latter transitions and the low-frequency modes of liquids is that there is not one type of transition with an inhomogeneous distribution, but a number of mechanical degrees of freedom (librational and translational modes with different center frequencies), corresponding to different transitions with their own distributions. These calcula-

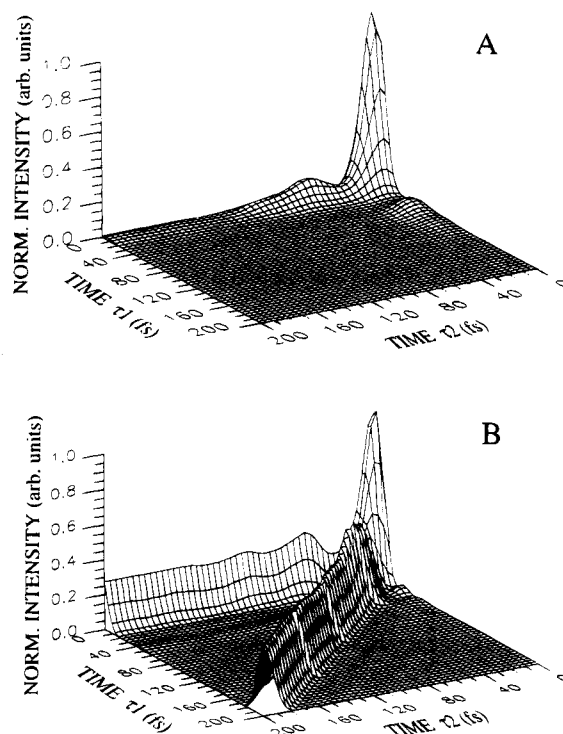


**Figure 2.**  $I^{(5)}(\tau_2, \tau_1)$  calculated response for the deconvolved water spectrum in the (A) homogeneous limit and (B) inhomogeneous limit. The delay between the excitations is  $\tau_1$ , and the probe delay from the final excitation is  $\tau_2$ .

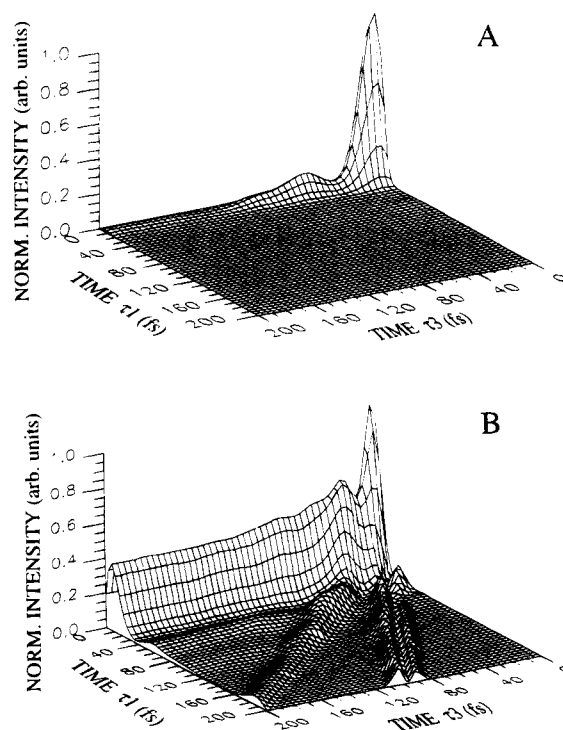


**Figure 3.**  $I^{(7)}(\tau_3, 0, \tau_1)$  calculated response for deconvolved water spectrum in the (A) homogeneous limit and (B) inhomogeneous limit. The delay between the excitations is  $\tau_1$ , and the probe delay from the final excitation is  $\tau_3$ .

tions show that even for a medium as complex as water the underlying inhomogeneity in its structure can be determined by higher-order Raman correlations. Close examination of Figures 2 and 3 shows that the exact form of the response is more complex than traditional echo phenomena due to inertial and potential interference effects of the different modes contributing to the induced polarization. Regardless, the echo-

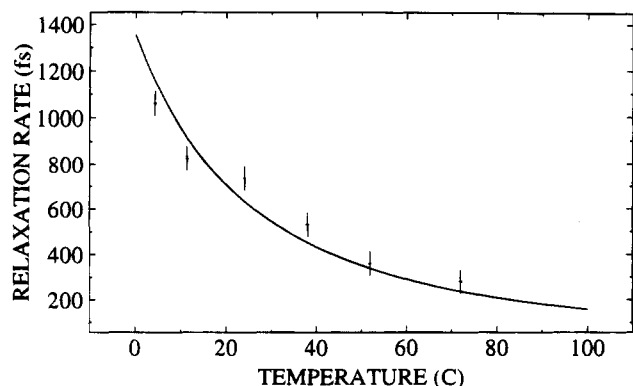


**Figure 4.** Temperature dependence for exponential relaxation observed in the OHD-OKE response of water. The exponential relaxation time as a function of temperature with fit assuming diffusive behavior described by the Stokes–Einstein–Debye model.

like behavior for the higher-order water response enables experimental determination of inhomogeneous dephasing mechanisms.

The actual water system would not be expected to have a static inhomogeneous component, as the liquid environment is constantly evolving. Instead, it is a question of the time scale required for the fluctuations in the liquid structure to alter the local environments and thus smear out any initial inhomogeneities.<sup>18</sup> The nonlinear response would therefore be expected to be intermediate between these two limits depending on the temporal separation of the excitation pulses relative to this fluctuation time scale. The intermediate case where both homogeneous and inhomogeneous contributions are present in the spectral density is an important consideration which is critical for making realistic comparisons to future experimental studies in this area.

In order to calculate the fifth-order intermediate response, a reasonable estimate for the homogeneous line width of liquid water is required. An upper limit on the time scale for the homogeneous relaxation can be obtained from OHD-OKE studies.<sup>19</sup> The diffusive portion of the response can be identified through temperature-dependent OHD-OKE studies. The experimental procedure followed is identical to that described before.<sup>16</sup> The water temperature was held constant to  $\pm 0.2$  °C in a flowing cell. The exponential time constant is shown in Figure 4 as a function of temperature. It can be seen that as the temperature is increased the exponential relaxation becomes shorter. This exponential relaxation can be interpreted with classical diffusive behavior by comparing these decays to the Stokes–Einstein–Debye diffusive model which predicts a relaxation rate which scales as  $\exp[-(kT/\eta V_{\text{eff}})t]$  where  $\eta$  is the bulk viscosity,  $T$  the temperature in kelvin, and  $V_{\text{eff}}$  the effective volume (see Figure 4). It can be seen that the diffusive model fits this portion of the relaxation. A detailed analysis of the temperature and isotope dependence of the spectral distribution will be forthcoming.<sup>20</sup> Here it is sufficient to identify the component which is diffusive and utilize the time constant extrapolated to 100 °C as an estimate for the upper limit of the homogeneous time constant (at standard atmospheric pressure). The value at the boiling point is utilized since to first order the correlation function is not implicitly dependent on temperature within the Brownian oscillator model.<sup>15</sup> Therefore, the relaxation rate at the boiling point will have minimal contributions from viscoelastic effects. These studies indicate that the exponential time constant extrapolated to 100 °C is  $150 \pm 30$  fs. With this in mind the spectral distribution shown in Figure 1 was fit using integral eqs 1 and 4. The homogeneous portion of the line width was taken to be Lorentzian with a damping

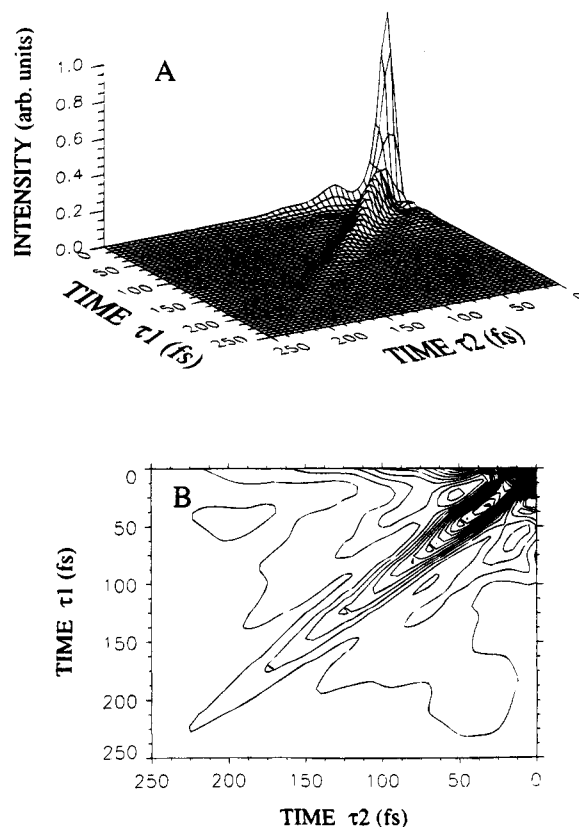


**Figure 5.**  $I^{(5)}(\tau_2, \tau_1)$  calculated response for deconvolved water spectrum in the intermediate case. The homogeneous contribution is assumed to be Lorentzian with a damping constant of  $70 \text{ cm}^{-1}$ , which is equivalent to the 150 fs time constant obtained from the time domain heterodyne OKE responses extrapolated to 100 °C. (A) Three-dimensional plot. (B) Contour plot of the square root of the intensity shown in (A).

( $\gamma_\alpha$ ) of  $70 \text{ cm}^{-1}$ , which corresponds to the 150 fs time constant. The exact functional dependence is not critical, and different forms produce the same qualitative results. The inhomogeneous distribution was assumed to have the same functional form as eq 13 where the parameters are adjusted to refit the distribution.

Using this fit to the spectral distribution, the intermediate fifth-order response was calculated using eqs 2 and 5. This response is shown in Figure 5A along with the contour plot (Figure 5B). The fifth-order response shows that at times much shorter than the homogeneous relaxation time the system behaves as in the purely inhomogeneous limit; i.e., there is a recurrence which is peaked at  $\tau_2 = \tau_1$  (the delay between the excitations). As the delay between the excitations is lengthened, the response breaks up into two components, one along the diagonal ( $\tau_2 = \tau_1$ ) and a second (seen in the lower right-hand quadrant of Figure 5B) which gravitates toward a constant delay from the second Raman excitation (as in the homogeneous limit). For a larger homogeneous line width the response is simply more highly damped along the diagonal, and it more quickly (and with greater relative amplitude) approaches a constant delay from the second Raman excitation.

The two components observed in this calculation have characteristics which have been seen using stochastic models<sup>18</sup> and classic Raman echo responses.<sup>7</sup> Within the stochastic model,<sup>18</sup> the response is found to approach a constant delay as the delay between the excitations is increased, relative to the liquid fluctuation time scale, while the classic Raman echo response<sup>7</sup> appears as a damped response at  $\tau_2 = \tau_1$ . Experimentally, since the temporal separation of the excitations and probe for such correlation experiments is limited to ap-

proximately 3 times the full width at half-maximum (fwhm) of the excitation pulse widths (due to coherent electronic effects), the damped response along  $\tau_2 = \tau_1$  is probably a better diagnostic of whether the liquid system has inhomogeneous contributions to the distribution.

These results are also applicable to other liquid systems. The general behavior is independent of the exact spectral distribution used in the calculation. It simply depends on the presence of both homogeneous and inhomogeneous contributions to the distribution. Therefore, qualitatively, fifth-order experiments on other liquid systems can be compared to these calculations.

### III. Concluding Remarks

The high-order correlation studies of low-frequency, intermolecular Raman-active modes are necessary to determine whether inhomogeneous contributions are present in liquid environments. The simple statement that the system is inhomogeneous has important implications for solvation dynamics. For example, such a result reinforces the idea that the spectral distribution obtained in OHD-OKE studies cannot be utilized *a priori* to directly calculate solvent relaxation. This connection can only be made if the system is completely homogeneous, which must be proven independently through correlation<sup>13,14</sup> and Raman echo<sup>21,22</sup> experiments. As opposed to intramolecular vibrations, the low-frequency Raman-active distribution for liquids is complex and cannot utilize two-level models to extract information on the homogeneous mechanisms. The analysis we have presented should form guidelines for future experiments directed at determining the dynamic structure of liquids. For example, using a three-pulse approach and differential detection to remove background scatter, a preliminary experimental study has found evidence for the higher-order signal in water, qualitatively similar to those calculated when inhomogeneous contributions are present.<sup>13</sup> These experimental studies need to be conducted with greater dynamic range and more selective phase matching conditions<sup>14</sup> to be definitive. However, this work and the above analysis are important steps in dissecting the spectral distribution to obtain important information on the dynamic structure of water.

The numerical calculations utilizing the off-resonance multimode Brownian oscillator model illustrate that differences in the homogeneous and inhomogeneous limits of the water intermolecular vibrational spectrum are observable in fifth- and seventh-order Raman spectroscopies. The intermediate case where both homogeneous and inhomogeneous components contribute to the spectrum indicates that at early times (relative to the homogeneous lifetime) the response behaves as in the purely inhomogeneous limit, while at later times the response

breaks up into two components, one damped along the diagonal ( $\tau_2 = \tau_1$ ) and the second which approaches a constant delay from the second Raman excitation. These higher-order Raman responses thus provide information on the homogeneous lifetime of the liquid environment and can readily determine whether the distribution has inhomogeneous contributions.

**Acknowledgment.** Support of this research was provided by the NSF Science and Technology Center on Photoinduced Charge Transfer (Grant CHE 9120001) and the General Electric Co.

### References and Notes

- (1) Mukamel, S. *Phys. Rep.* **1982**, *93*, 1.
- (2) Schweizer, K. S.; Chandler, D. *J. Chem. Phys.* **1982**, *76*, 2296.
- (3) Kivelson, B.; Madden, P. A. *Annu. Rev. Phys. Chem.* **1980**, *31*, 523. Yarwood, J. *Annu. Rev. Prog. Chem.* **1982**, *79C*, 157.
- (4) Yan, Y.-X.; Gamble, Jr., E. B.; Nelson, K. A. *J. Chem. Phys.* **1985**, *83*, 5391.
- (5) McMorrow, D.; Lotshaw, W. T.; Kenny-Wallace, G. A. *IEEE Quantum Electron.* **1988**, *24*, 443.
- (6) Fried, L. E.; Mukamel, S. *Adv. Chem. Phys.* **1993**, *84*, 435.
- (7) Loring, R. F.; Mukamel, S. *J. Chem. Phys.* **1985**, *83*, 2116.
- (8) Maroncelli, M.; Fleming, G. R. *J. Chem. Phys.* **1988**, *89*, 5044.
- (9) Franks, F. In *Water, a Comprehensive Treatise*; Franks, F., Ed.; Plenum Press: New York, 1972; Vol. 1, Vols. 1-7, 1972-1982.
- (10) Ohmine, I.; Tanaka, H. *Chem. Rev.* **1993**, *93*, 2545.
- (11) Cho, M.; Fleming, G. R.; Saito, S.; Ohmine, I.; Stratt, R. M. *J. Chem. Phys.* **1994**, *100*, 6672.
- (12) Sastry, S.; Stanley, H. E.; Sciortino, F. *J. Chem. Phys.* **1994**, *100*, 5361.
- (13) Palese, S.; Buontempo, J. T.; Tanimura, Y.; Mukamel, S.; Miller, R. J. D.; Lotshaw, W. T. In *Ultrafast Phenomena IX*; Vol. 7., 1994 OSA Technical Digest Series; Optical Society of America: Washington, DC, 1994; WC21.
- (14) Tominaga, K.; Naitoh, Y.; Kang, T. J.; Yoshihara, K. In *Ultrafast Phenomena IX*; Vol. 7., 1994 OSA Technical Digest Series; Optical Society of America: Washington, DC, 1994; PD7.
- (15) Tanimura, Y.; Mukamel, S. *J. Chem. Phys.* **1993**, *99*, 9496.
- (16) Palese, S.; Schilling, L.; Miller, R. J. D.; Staver, R.; Lotshaw, W. T. *J. Phys. Chem.* **1994**, *98*, 6308.
- (17) Walrafen, G. E.; Fischer, M. R.; Hokmabadi, M. S.; Yang, W. H. *J. Chem. Phys.* **1986**, *85*, 6970. Walrafen, G. E.; Hokmabadi, M. S.; Yang, W. H. *J. Chem. Phys.* **1988**, *88*, 4555.
- (18) Nibbering, E. T. J.; Wiersma, D. A.; Duppen, K. In *Coherence Phenomena in Atoms and Molecules in Laser Fields*; Bandrauk, A. D., Wallace, S. C., Eds.; Plenum Press: New York, 1992; pp 377-391.
- (19) McMorrow, D.; Lotshaw, W. T. *Chem. Phys. Lett.* **1991**, *178*, 69.
- (20) Palese, S.; Schilling, L.; Miller, R. J. D.; Staver, R.; Lotshaw, W. T., to be submitted for publication.
- (21) Vanden Bout, D.; Muller, L. J.; Berg, M. *Phys. Rev. Lett.* **1991**, *67*, 3700.
- (22) Inaba, R.; Tominaga, K.; Tasumi, M.; Nelson, K. A.; Yoshihara, K. *Chem. Phys. Lett.* **1993**, *211*, 183.
- (23) By assuming specific functional forms for  $J$  and  $S$ , it may be possible to fit a given spectral density and obtain  $J$  and  $S$ . This procedure depends, however, on the assumptions made in modeling and requires additional information about the system. A single experiment does not itself directly distinguish between the two (ref 6).